JMEPEG (2016) 25:359–364
DOI: 10.1007/s11665-015-1856-8

1059-9495/$19.00

Regulation Mechanism of Novel Thermomechanical Treatment on Microstructure and Properties in Al-Zn-Mg-Cu Alloy

Zhiguo Chen, Jieke Ren, Jishuai Zhang, Jiqiang Chen, and Liang Fang

(Submitted June 25, 2015; in revised form November 12, 2015; published online December 28, 2015)

Scanning electron microscopy, transmission electron microscopy, tensile test, exfoliation corrosion test, and slow strain rate tensile test were applied to investigate the properties and microstructure of Al-Zn-Mg-Cu alloy processed by final thermomechanical treatment, retrogression reaging, and novel thermomechanical treatment (a combination of retrogression reaging with cold or warm rolling). The results indicate that in comparison with conventional heat treatment, the novel thermomechanical treatment reduces the stress corrosion susceptibility. A good combination of mechanical properties, stress corrosion resistance, and exfoliation corrosion resistance can be obtained by combining retrogression reaging with warm rolling. The mechanism of the novel thermomechanical treatment is the synergistic effect of composite microstructure such as grain morphology, dislocation substructures, as well as the morphology and distribution of primary phases and precipitations.

Keywords Al-Zn-Mg-Cu alloy, corrosion resistance, microstructure, thermomechanical treatment

1. Introduction

With the fast development of aerospace industry, great efforts are made to improve the comprehensive properties of aluminum alloys. With its high specific strength, good formability, and welding performance, Al-Zn-Mg-Cu alloy has long been extensively applied in aerospace industry, however, its susceptibility to stress corrosion and exfoliation corrosion has become a severe disadvantage (Ref 1). Thus, processing techniques that improve the comprehensive properties of Al-Zn-Mg-Cu alloy, such as retrogression reaging (RRA) and final thermomechanical treatment (FTMT), have drawn wide attention (Ref 2-4). Research on Al-Zn-Mg-Cu alloy showed that RRA process is capable of granting both high strength and good corrosion resistance (Ref 3). Besides, some research showed that by applying FTMT, the fatigue resistance of Al-Zn-Mg-Cu alloy can be improved by 25% (Ref 5), while other researches showed that the strength of 7475 alloy is improved under thermomechanical treatment with 100 °C pre-aging, and its fatigue life is also 19.5% longer than that of T6 alloy (Ref 6). Previous work of our research showed that novel thermomechanical treatment improves the comprehensive properties of 2E12 alloy (Ref 7), including strength-plasticity combination and fatigue crack propagation resistance. The thermomechanical treatment for Al-Zn-Mg-Cu alloy in existence generally focuses on pre-deformation before aging (Ref 8, 9), however, there is little research on thermomechanical treatment with deformation between different aging stages or after retrogression. Besides, the effect and mechanism of thermomechanical treatment on Al-Zn-Mg-Cu alloy still need further investigation. The effect of thermomechanical treatment on the properties and microstructure of Al-Zn-Mg-Cu alloy will be systematically studied in this work.

2. Experimental Methods

A cold-rolled Al-Zn-Mg-Cu alloy plate with a thickness of 2 mm provided by Southwest Aluminium (Group) CO. was used in this investigation. The specific content of the alloy was Al-5.13Zn-2.58 Mg-1.42Cu -0.21Cr-0.27Si-0.12Fe (wt.%). The samples were solution treated at 470 °C for 1 h, then quenched in water to room temperature. The subsequent heat treatment processes for different samples are shown in Table 1, the warm rolling was performed at 200 °C. The tensile tests were performed on a materials testing machine (MTS 858) with a gauge length of 20 mm at a constant strain rate of 8×10^{-4} s^{-1}, the tensile tests were carried out according to ISO6892.1-2009. The exfoliation corrosion test was carried out according to ASTM-G34-01, the corrosive medium is exfoliation corrosion test (EXCO) solution (4.0 mol/L NaC1 + 0.1 mol/L HNO_3 + 0.4 mol/L KNO_3, pH = 0.4), the ratio between the volume of solution and sample

Zhiguo Chen, School of Materials Science and Engineering, Central South University, Changsha 410083, People's Republic of China; Light Alloy Research Institute, Central South University, Changsha 410083, People's Republic of China; and Department of Mechanical and Electrical Engineering, Hunan University of Humanities, Science and Technology, Loudi 417000, People's Republic of China and **Jieke Ren, Jishuai Zhang, Jiqiang Chen,** and **Liang Fang**, School of Materials Science and Engineering, Central South University, Changsha 410083, People's Republic of China and Light Alloy Research Institute, Central South University, Changsha 410083, People's Republic of China. Contact e-mails: hngary@163.com, renjieke@126.com, zhangjscsu@163.com, 343167526@qq.com, 343167526@qq.com, and zgchen@mail.csu.edu.cn.

experimental area is 15 mL/cm^2. Exfoliation corrosion rating can be summarized by the EXCO rating scales: ED (Extremely severe exfoliation) > EC > EB > EA (Slight exfoliation) > PC (Severe pitting) > PB > PA (Slight pitting) > N (no obvious exfoliation), rate P is used to indicate pitting when evaluating pitting degree is unnecessary. The slow strain rate tensile test was performed on materials testing machine (WDML-1) in ambient air or 3.5%NaCl + 0.5%H_2O_2 aqueous solution, the gauge size of the samples is 20 mm × 6 mm × 2 mm, and the strain rate is 2×10^{-6} s^{-1}. The stress corrosion sensitivity index I_{SSRT} is an important criterion for evaluating the stress corrosion susceptibility, and its expression is as follows (Ref 10):

$$I_{SSRT} = 1 - [\sigma_{fw} \times (1 + \delta_{fw})]/[\sigma_{fA} \times (1 + \delta_{fA})].$$

In this expression, σ_{fw} is the fracture strength in environment medium (MPa); δ_{fw} is the elongation in environment medium (%); σ_{fA} is the fracture strength in inert medium (MPa); δ_{fA} is the elongation in inert medium (%). The value of I_{SSRT} increases from 0 to 1, representing the growing of stress corrosion susceptibility.

The SEM observations were performed on Sirion 200 field emission scanning microscope, with an operating voltage of 25 kV. The TEM observations were performed on Tecnai G^2 20 transmission electron microscope, with an operating voltage of 200 kV. The specimens for TEM observation were prepared by the standard twin jet electro-polishing method, using a solution of methanol and nitric acid (3:1 in volume) at below −25 °C.

3. Results and Discussion

The tensile properties of the Al-Zn-Mg-Cu alloy processed by different thermomechanical treatments are shown in Table 1 and Fig. 1, with T6 and T8 alloy as control group. The yield strength (YS) is the load corresponding to $\sigma_{0.2}$, while the

Table 1 Tensile property results of Al-Zn-Mg-Cu alloy under different heat treatments

State	Heat treatment	$\sigma_{0.2}$, MPa	σ_b, MPa	δ, %
T6	120 °C, 24 h	489	578	14.8
T8	9%CR + 120 °C, 24 h	497	571	12.7
RRA	T6 + 200°C, 10 min + T6	489	576	13.4
FTMT (CR)	120°C,4 h + 9% CR + 120°C, 10 h	528	609	12.3
FTMT (WR)	120°C,4 h + 9%WR +120°C, 10 h	537	601	13.2
RRA (CR)	T6 + 200°C, 10 min + 9% CR + T6	533	616	11.5
RRA (WR)	T6 + 200 °C, 10 min + 9% WR + T6	526	601	13.3

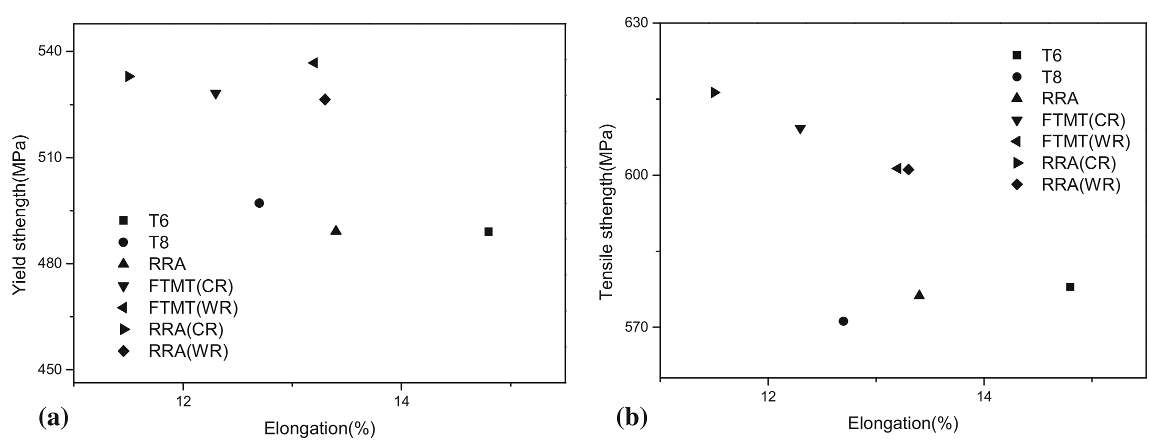

Fig. 1 The tensile properties of Al-Zn-Mg-Cu alloy processed under different treatments: (a) yield strength-elongation; (b) tensile strength-elongation

Table 2 Slow strain tensile properties of Al-Zn-Mg-Cu alloy

	σ_b, MPa			δ, %			
Alloy	Air	Sol	σ_b loss, %	Air	Sol	δ Loss, %	I_{SSRT}
T6	582	528	9.4	21.7	9.3	57.1	0.187
T8	577	567	1.8	21.7	10.4	51.9	0.109
RRA	568	551	3.1	19.3	15.0	21.9	0.064
FTMT (CR)	592	564	4.7	18.2	17.1	5.8	0.055
RRA (CR)	582	558	4.2	18.9	16.8	11.3	0.059
RRA (WR)	593	582	1.9	18.2	15.1	17.1	0.044

Table 3 Grade of exfoliation corrosion of alloy under different heat treatments

	Corrosion exposure time, h					
State	**4**	**8**	**12**	**18**	**24**	**48**
T6	N	N+	P	EA	EB	EC
T8	N	N	PA	PB	PB	EA
RRA	N	N	N	PA	PA+	PB−
FTMT (CR)	N	P+	EA	EA	EA+	EB+
FTMT (WR)	N	N	PA−	PA	PA+	PB
RRA (CR)	N	N	N+	PA	PA	PC+
RRA (WR)	N	N	PA	PA	PB−	PC

Pitting on the surface; *PA*− slight pitting; PB− moderate pitting; PC− severe pitting; EA− slight exfoliation; EB− moderate exfoliation; EC− severe exfoliation; E − extremely severe exfoliation. + and − indicates increased or decreased degree

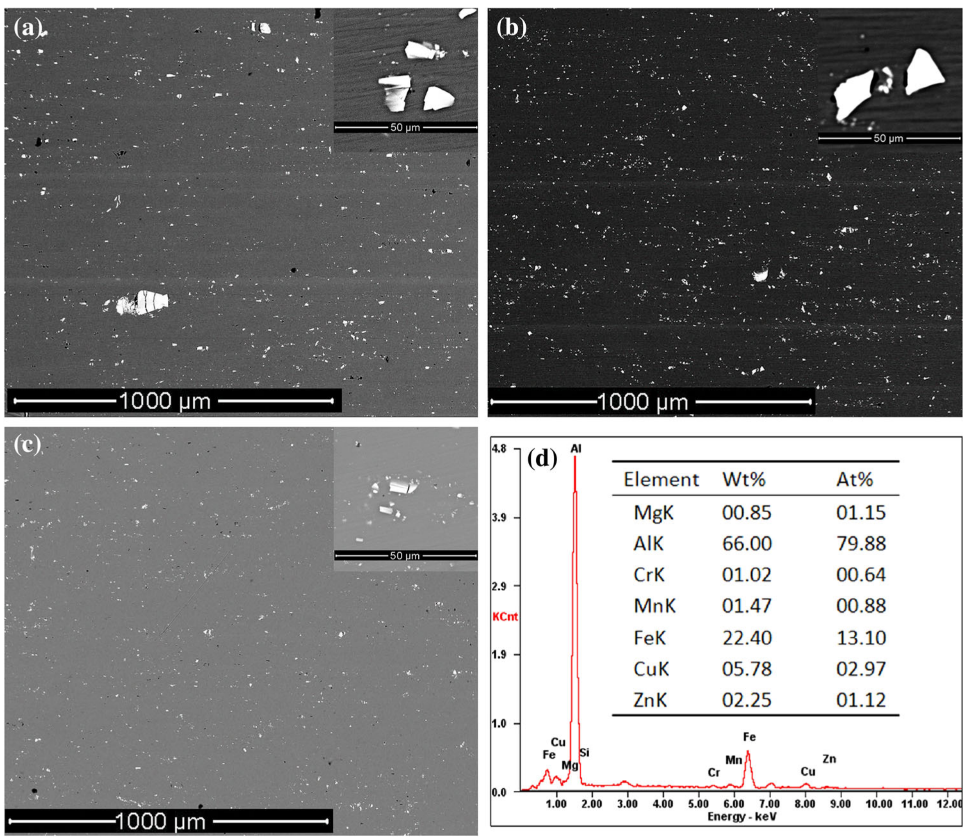

Fig. 2 SEM morphology of Al-Zn-Mg-Cu alloy: (a) T6; (b) RRA; (c) RRA(WR); (d) EDS analysis

ultimate tensile strength (UTS) is the maximum load before failing. The deformation process mentioned below is cold rolling (CR) or warm rolling (WR) at 200 °C. It can be concluded that the strength of the alloy can be increased by both FTMT (FTMT(CR), FTMT(WR)) and novel thermomechanical treatments (RRA(CR) RRA(WR)); the samples with warm rolling as deformation only suffered minor elongation loss, while the samples processed by cold rolling suffered more elongation loss.

The slow strain tensile properties of different alloys are shown in Table 2. It is shown in Table 2 that T6 samples suffered major strength and elongation loss. Although T8 samples only suffered minor strength loss, the elongation loss is significant. The elongation loss of the thermomechanical treatment processed Al-Zn-Mg-Cu samples is lower than that of the samples processed by conventional heat treatment (T6, T8 and RRA), besides, the elongation loss of the FTMT(CR) samples is the lowest. The stress corrosion susceptibilities of the thermomechanical treatment processed alloys are also lower than those of the alloys under conventional heat treatment, as indicated by I_{SSRT}. As the thermomechanical treatment shattered the coarse primary phases, the micro-battery effect is weakened, and the pitting susceptibility is decreased (Ref 11). Besides, the fibrous grain structure of the rolled alloy hindered the propagation of the stress corrosion crack (Ref 12). As a result, Al-Zn-Mg-Cu alloy processed by RRA(WR) has the best stress corrosion resistance.

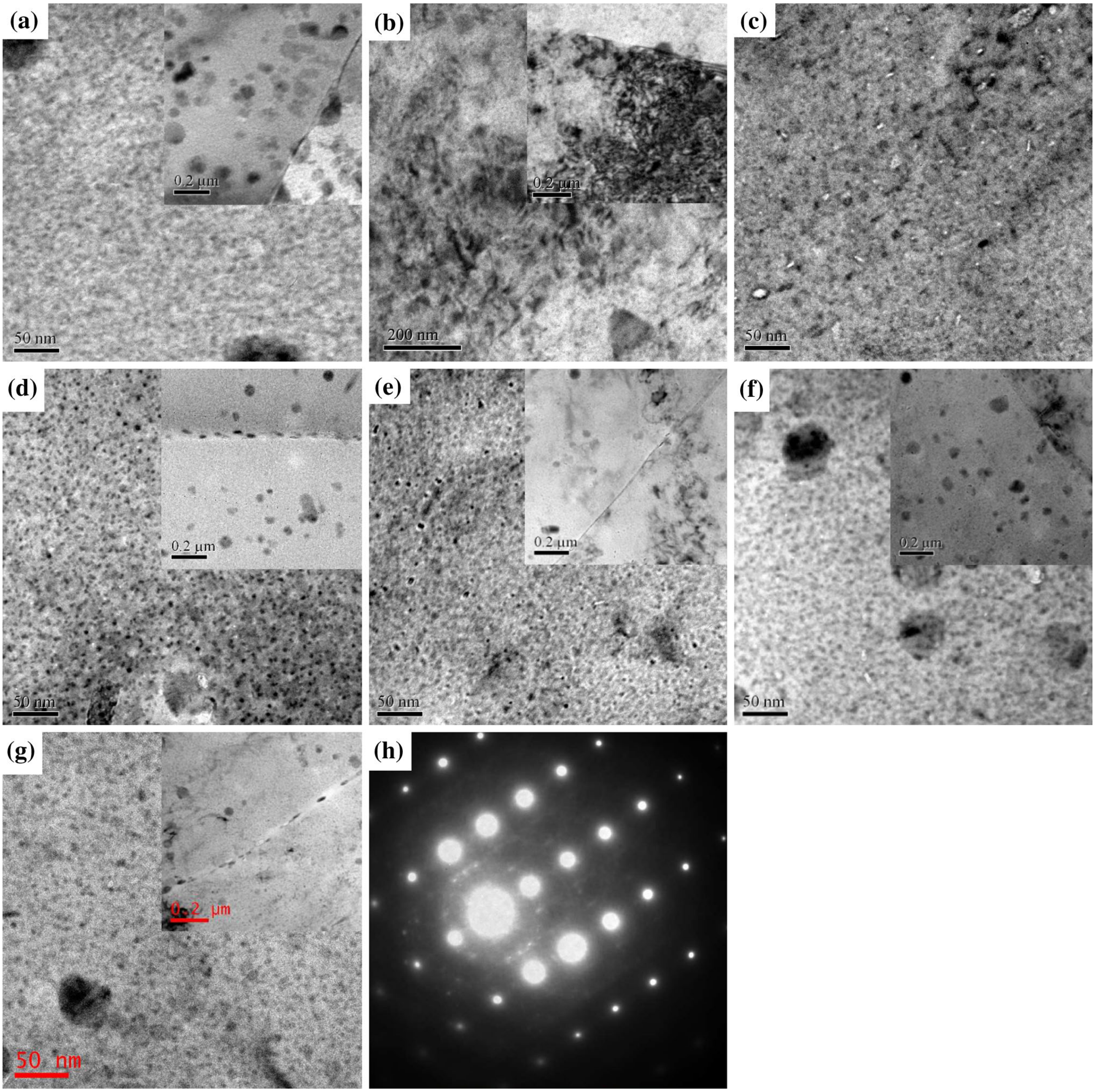

Fig. 3 TEM morphology of Al-Zn-Mg-Cu alloy under different treatments: (a) T6; (b) T8; (c) T8 state precipitates in the matrix; (d) RRA; (e) FTMT (CR); (f) RRA (CR); (g) RRA(WR); (h) the diffraction pattern of η′ phase in the matrix, taken along $[112]_{Al}$ zone axis

Exfoliation corrosion rating of Al-Zn-Mg-Cu alloy under different heat treatments is shown in Table 3. It is well accepted that coarse and discontinuous grain boundary precipitates are beneficial to the exfoliation corrosion resistance (Ref 13, 14), as the formation of anode corrosion path is restrained. As a result, the stress corrosion resistance is also increased by the novel thermomechanical treatment. In this paper, the morphology of grain boundary precipitates is also in agreement with the corresponding exfoliation corrosion resistance. The RRA is more favorable to the exfoliation corrosion resistance of the alloy than RRA(CR) or RRA(WR), as rolling increases the aspect ratio of the grain, which increases the exfoliation susceptibility of the corresponding alloy.

The SEM morphology of T6, RRA and RRA(WR) samples is shown in Fig. 2(a) to (c), random distribution of white primary phases can be observed in the matrix. The EDS analysis of the coarse phase is shown in Fig. 2(d), the component of the phase is AlFeCu, thus the primary phase is likely the $(Al,Cu)_6(Fe,Cu)$ Al_6Fe or Al_7Cu_2Fe phase (Ref 15). The primary phase will serve as cathode relative to the matrix, and corrosion will preferentially occur near the primary phase (Ref 16, 17). The primary phases are coarse and concentrated in both T6 and RRA samples by contrast. By comparing Fig. 2(a) and (b), it can be concluded that aging has no obvious effect on the morphology and distribution of the primary phase, as the primary phase hardly dissolves into the matrix at elevated temperature. It can also be observed in Fig. 2(c) that the primary phases are shattered and redistributed randomly during deformation in RRA(WR) alloy (Ref 11).

The TEM morphology of Al-Zn-Mg-Cu alloy under different treatments is shown in Fig. 3. In Fig. 3(a), fine and dispersed η′ phase can be observed in the matrix, while contiguous precipitates can be observed on the grain boundary; there is also obvious precipitate-free zone (PFZ) near the grain boundary. A high density of dislocations can be observed in Fig. 3(b), since the dislocations are favorable sites for the formation of η phase (Ref 18), coarse equilibrium η phase as well as η′ phase can be observed in the matrix, as it is shown in Fig. 3(c); on the other hand, the grain boundary precipitates of the alloy are also less contiguous. No obvious PFZ can be observed, as the dislocations may serve as the path for solute atom diffusion from matrix to grain boundary. It can be observed in 3-(d) that the η′ phase in the matrix is not as fine as that of T6 sample, and the grain boundary precipitates are much coarser, the spans in between are also greater. For the alloys under thermomechanical treatment [Fig. 3(e) to (g)], the η′ phase in the matrix is fine and dispersed. In Fig. 3(e), the grain boundary precipitates are fine and contiguous; in Fig. 3(f) and (g), the grain boundary precipitates are coarse and discontinuous. It can be concluded that the alloy under RRA(WR) treatment processes an outstanding combination of tensile properties and corrosion resistance, as the η′ phase in matrix is both fine and dispersed, while the grain boundary precipitates are coarse and discontinuous.

For T8 samples, though the dislocations generated by the deformation caused stress concentration, increasing the strength while decreasing the elongation, the strengthening effect of the coarse η phase is not as great as that of the fine and dispersed η′ phase, thus the strength of T8 samples is close to that of the T6 samples. Pre-aging will lead to the precipitation of the fine G.P. zones and η′ phase. It is generally accepted that in RRA process, GP zones and fine η′ phase will partially dissolute into the matrix during retrogression and re-precipitate during the re-aging, while discontinuous η phase on the grain boundaries continues to grow and coarsen (Ref 19, 20). Warm rolling causes the dislocations to be uniformly distributed and reduces the dislocation density, increasing the plasticity of the alloy at the cost of a slight decrease in strength (Ref 21, 22). Besides, warm rolling has significant effect on the precipitation of the alloy. In the warm rolling process, the G.P. zones and fine η′ phase will partly dissolve into the matrix at 200 °C, while the grain boundary precipitates will continue to coarsen, resulting in better corrosion resistance. It can be concluded that novel thermomechanical treatment utilizes the synergistic effect of composite microstructure including dislocations, primary phases, and precipitations, granting an optimum combination of deformation strengthening and precipitation strengthening.

4. Conclusions

(1) FTMT(WR) and RRA(WR) can increase the strength of Al-Zn-Mg-Cu alloy while retaining its ductility. However, FTMT(CR) and RRA(CR) can only increase the strength of the alloy without retaining the elongation.
(2) RRA(WR) greatly reduces the stress corrosion susceptibility of Al-Zn-Mg-Cu alloy, in comparison with conventional heat treatment and FTMT.
(3) RRA(CR) and RRA(WR) greatly improve the exfoliation corrosion resistance of Al-Zn-Mg-Cu alloy, while FTMT(CR), T6, and T8 samples suffer severe exfoliation corrosion.
(4) The mechanism of the novel thermomechanical treatment is a synergistic effect of the composite microstructure, as the dislocation substructure generated during deformation is strongly affect by precipitation in the aging process, and it in turn affects the precipitation of subsequent aging.

Acknowledgments

This work is financially supported by Australia-China Special Fund (Grant No. 51011120052) and the National Natural Science Foundation of China (Grant No. 50871123).

References

1. T. Marlaud, A. Deschamps, F. Bley, W. Lefebvrec, and B. Baroux, Influence of Alloy Composition and Heat Treatment on Precipitate Composition in Al-Zn-Mg-Cu Alloys, *Acta Mater.*, 2010, **58**(1), p 248–260
2. J.K. Park and A.J. Ardell, Effect of Retrogression and Reaging Treatments on the Microstructure of Al 7075-T65, *Metall. Trans. A*, 1984, **15**, p 1531–1539
3. B. Cina, Reducing the Susceptibility of Alloys, Particularly Aluminium Alloys, to Stress Corrosion Cracking: U.S. Patent, 3856584. 1974-12-24
4. Y.P. Xiao, Q.L. Pan, W.B. Li, X.Y. Liu, and Y.B. He, Influence of Retrogression and Reaging Treatment on Corrosion Behaviour of an Al-Zn-Mg-Cu Alloy, *Mater. Design*, 2011, **32**(4), p 2149–2156
5. F. Ostermann, Improved Fatigue Resistance of Al-Zn-Mg Alloys Through Thermomechanical Processing, *Mater. Trans.*, 1971, **2**(10), p 2897–2902
6. M.T. Jahn and J. Luo, Tensile and Fatigue Properties of a Thermomechanically Treated 7475 Aluminium Alloy, *J. Mater. Sci.*, 1988, **23**(11), p 4115–4120
7. Ren Jie-ke, Chen Zhi-guo, Huang Yu-jin, and Zhang Ji-shuai, Effect of New Thermomechanical Treatment on Microstructure and Properties of 2E12 Aluminum Alloy, *Chin. J. Nonferrous Met.*, 2014, **24**(3), p 643–650 ((in Chinese))
8. D. Wang and Z.Y. Ma, Effect of Prestrain on Microstructure and Stress Corrosion Cracking of Overaged 7050 Aluminum Alloy, *J. Alloys Compd.*, 2009, **469**(1/2), p 445–450
9. N.M. Han, X.M. Zhang, S.D. Liu, and B. Ke, Effects of Prestretching and Ageing on the Strength and Fracture Toughness of Aluminum Alloy 7050, *Mater. Sci. Eng. A*, 2011, **528**(10/11), p 3714–3721
10. Liu Ji-hua, Li Di, and Liu Pei-ying, Effect of Ageing and Retrogression Treatments on Mechanical and Corrosion Properties of 7075 Aluminum Alloy, *Trans. Mater. Heat Treat.*, 2002, **23**(1), p 50–53
11. R. Ayer, J.Y. Koo, J.W. Steeds, and B.K. Park, Microanalytical Study of the Heterogeneous Phases in Commercial Al-Zn-Mg-Cu Alloys, *Metall. Trans. A*, 1985, **16(A)**, p 1925–1936
12. F. Andreatta, H. Terryn, and J.H.W. de Wit, Effect of Solution Heat Treatment on Galvanic Coupling Between Intermetallics and Matrix in AA7075-T6, *Corros. Sci.*, 2003, **45**(8), p 1733–1746
13. L.P. Huang, K.H. Chen, S. Li, and M. Song, Influence of High-Temperature Pre-precipitation on Local Corrosion Behaviors of Al-Zn-Mg Alloy, *Scr. Mater.*, 2007, **56**(4), p 305–308
14. M. Dixit, R.S. Mishra, and K.K. Sankaran, Structure-Property Correlations in Al 7050 and Al 7055 High-Strength Aluminum Alloys, *Mater. Sci. Eng. A*, 2008, **478**(1-2), p 163–172
15. Y. Reda, R. Abdel-Karim, and I. Elmahallawi, Improvements in Mechanical and Stress Corrosion Cracking Properties in Al-Alloy 7075 Via Retrogression and Reaging, *Mater. Sci. Eng. A*, 2008, **485**(1-2), p 468–475

16. G. Waterloo, V. Hansen, J. Gjønnes, and S.R. Skjervold, Effect of Predeformation and Pre-aging at Room Temperature in Al-Zn-Mg-(Cu, Zr) Alloys, *Mater. Sci. Eng. A*, 2001, **303**(1), p 226–233
17. N. Birbilis, M.K. Cavanaugh, and R.G. Buchheit, Electrochemical Behavior and Localized Corrosion Associated with Al_7Cu_2Fe Particles in Aluminum Alloy 7075-T651, *Corros. Sci.*, 2006, **48**(12), p 4202–4215
18. N. Enung and P. Sunara, Improvement of Stress Corrosion Resistance in Aluminum Alloy 7075 through Retrogression and Re-aging Modification, *Adv. Mater. Res.*, 2013, **789**, p 467–475
19. G. Peng, K. Chen, S. Chen, and H. Fang, Influence of Repetitious-RRA Treatment on the Strength and SCC Resistance of Al-Zn-Mg-Cu Alloy, *Mater. Sci. Eng. A*, 2011, **528**(12), p 4014–4018
20. J.F. Li, Z.W. Peng, C.X. Li, Z.Q. Jia, W.J. Chen, and Z.Q. Zheng, Mechanical Properties, Corrosion Behaviors and Microstructures of 7075 Aluminium Alloy with Various Aging Treatments, *Trans. Nonferrous Met. Soc. China*, 2008, **18**(4), p 755–762
21. U.J. Gang, S.H. Lee, and W.J. Nam, The evolution of Microstructure and Mechanical Properties of a 5052 Aluminium Alloy by the Application of Cryogenic Rolling and Warm Rolling, *Mater. Trans.*, 2009, **50**(1), p 82–86
22. P. Nageswara rao and R. Jayaganthan, Effects of Warm Rolling and Ageing After Cryogenic Rolling on Mechanical Properties and Microstructure of Al 6061 Alloy, *Mater. Des.*, 2012, **39**, p 226–233